are van der Waals contacts [2·516 (5)||2·489 (4) Å] between the H(2) atom of the ammonium $NH_4$ group above the $IO_6$ octahedron and three near O atoms.

## Conclusions

Both structures were refined with anisotropic temperature parameters including H atoms. For both structures the extinction corrections amount to more than 70%, *i.e.* less than 30% of the kinematical intensity was really measured for the strongest reflections. Choosing a smaller sample for the deuterated substance did not help in this respect and we think that too high a quality of the crystals, rather than their size, was responsible for the magnitude of the extinction effects.

Although the degree of deuteration determined by infrared spectroscopy (87 ± 1%) differs by 8·5% from our value of 95·5 ± 2·5%, computed from resultant least-squares values of $b_D$, the difference amounts to $\sim 3\sigma$ only and it is encouraging that, even though the scale factor, the refined scattering lengths $b_D$ and the thermal parameters were highly correlated, no scattering length $b_D$ of the substituted D atoms ever exceeded during the refinement the value $b_D = 6{\cdot}67$ fm for pure deuterium. Therefore we believe that the positional parameters of all H and D atoms, including the dynamical disorder in the interlayer $O-H_{disordered}\cdots O$ hydrogen bonds, are well established by this study.

We thank W. Huber, Laboratory of Solid State Physics, ETH, for supplying us with the crystals used in this study, R. Keil, Department of Chemistry of the Swiss Federal Institute for Reactor Research, for the infrared spectroscopic determination of the deuterium contents in the deuterated crystal, Dr W. Petter, Institute of Crystallography, ETH, for using the Syntex $P2_1$ four-circle X-ray diffractometer for accurate unit-cell determination of both substances and for his help, Drs R. Kind and H. Arend, Laboratory of Solid State Physics, ETH, for numerous discussions and Professors W. Hälg and A. Niggli for their continuous interest and support.

## References

BACON, G. E. (1972). *Acta Cryst.* A**28**, 357–358.
BUSING, W. R., MARTIN, K. O. & LEVY, H. A. (1962). *ORFLS*. Report ORNL-TM-305. Oak Ridge National Laboratory, Tennessee.
BUSING, W. R., MARTIN, K. O. & LEVY, H. A. (1964). *ORFFE*. Report ORNL-TM-306. Oak Ridge National Laboratory, Tennessee.
GRÄNICHER, H., KIND, R., MEIER, W. M. & PETTER, W. (1968). *Helv. Phys. Acta*, **41**, 843–854.
HAMILTON, W. C. & IBERS, J. A. (1968). *Hydrogen Bonding in Solids*, p. 104. Amsterdam & New York: Benjamin.
HELMHOLZ, L. (1937). *J. Am. Chem. Soc.* **59**, 2036–2039.
*International Tables for X-ray Crystallography* (1952). Vol. I, pp. 20, 53 and 253. Birmingham: Kynoch Press.
JOHNSON, C. K. (1969). *Acta Cryst.* A**25**, 187–194.
JOHNSON, C. K. (1971). *ORTEP* II. Report ORNL-3794, revised. Oak Ridge National Laboratory, Tennessee.
KIND, R. (1971). *Phys. Kondens. Mater.* **13**, 217–245.
RÜEGG, A. (1977). Thesis No. 5908, Eidg. Technische Hochschule, Zürich, Switzerland.
STEWART, J. M., KRUGER, G. J., AMMON, H. L., DICKINSON, C. & HALL, S. R. (1972). The XRAY system – version of June 1972. Tech. Rep. TR-192. Computer Science Center, Univ. of Maryland, College Park, Maryland.
ZACHARIASEN, W. H. (1967). *Acta Cryst.* **23**, 558–564.

*Acta Cryst.* (1980). B**36**, 1032–1040

# Hydrogen Bond Studies. CXXXVIII.* Neutron Diffraction Studies of $LiNO_3.3H_2O$ at 120 and 295 K

BY KERSTI HERMANSSON, JOHN O. THOMAS AND IVAR OLOVSSON

*Institute of Chemistry, Uppsala University, Box* 531, *S*-751 21 *Uppsala, Sweden*

(*Received* 30 *October* 1979; *accepted* 12 *December* 1979)

## Abstract

$LiNO_3.3H_2O$ has been studied by neutron diffraction at 120 and 295 K. The final $R_{w,F^2}$ values are 4·5% (120 K) and 4·9% (295 K). The crystal structure found in a previous room-temperature X-ray study is confirmed: one water molecule is involved in six hydrogen bonds; the other independent water molecule in the structure has a tetrahedral environment comprising two $Li^+$ ions and two medium–strong hydrogen bonds. The four different O···O hydrogen-bond lengths increase by 0·02–0·03 Å going from 120 to 295 K. The mean-

* Part CXXXVII: Lundgren & Taesler (1979).

0567-7408/80/051032-09$01.00

square amplitudes of vibration for the N and O atoms are found to be closely proportional to temperature. For the H and Li atoms the vibrational amplitudes are less sensitive to temperature. {Crystal data: space group *Cmcm*, $Z = 4$; at 120 K $a = 6{\cdot}713$ (7), $b = 12{\cdot}669$ (4), $c = 5{\cdot}968$ (5) Å; at 295 K [Hermansson, Thomas & Olovsson (1977), *Acta Cryst.* B**33**, 2857–2861] $a = 6{\cdot}8018$ (4), $b = 12{\cdot}7132$ (9), $c = 5{\cdot}9990$ (4) Å.}

## Introduction

The purpose of the two experiments reported in this paper was to obtain accurate positional and thermal parameters for $LiNO_3.3H_2O$ for use in subsequent electron-density studies at 120 and 295 K (Hermansson, Thomas & Olovsson, 1980). We have also studied the variation of thermal vibration with temperature and compared it with that deduced from spectroscopic measurements. The room-temperature structure has previously been determined by Hermansson, Thomas & Olovsson (1977). This work forms part of a project directed towards the study of electron density in simple hydrates.

## Experimental

Crystals of $LiNO_3.3H_2O$ were grown by evaporation from an aqueous solution of lithium nitrate. The flat irregular crystal used in the room-temperature study was bounded by ten faces; maximum and minimum distances between parallel faces were 6·0 and 1·8 mm, respectively. A rod-shaped crystal of length 5·5 mm in the **c** direction and cross-section about 1·0 mm$^2$ was used for the low-temperature study. The deliquescent crystals were glued with Araldite on to an aluminum pin and sealed in a thin-walled quartz-glass bulb.

X-ray photographs taken at 120 K confirmed the systematic extinctions and the symmetry of the diffraction pattern found at 295 K and were consistent with three space groups: *Cmcm*, $Cmc2_1$, and $C2cm \equiv Ama2$. Crystal data are presented in Table 1.

Table 1. *Crystal data for* $LiNO_3.3H_2O$

| | 120 K | 295 K |
|---|---|---|
| FW | 123·00 | |
| Space group | *Cmcm* | |
| $Z$ | 4 | |
| M.p. (K) | 303·1 | |
| $a$ (Å) | 6·713 (7)* | 6·8018 (4)† |
| $b$ (Å) | 12·669 (4) | 12·7132 (9) |
| $c$ (Å) | 5·968 (5) | 5·9990 (4) |
| $V$ (Å$^3$) | 507·6 | 518·75 |
| $D_x$ (Mg m$^{-3}$) | 1·609 | 1·575 |

* Obtained from 22 reflections measured on a CAD-4 diffractometer at 120 K.

† Hermansson, Thomas & Olovsson (1977).

### *The* 120 K *data; data collection and reduction*

Experimental details for the neutron data collections are summarized in Table 2. The low temperature was obtained with an Air Products and Chemicals Inc., Model CS-1003 Displex® closed-cycle cooling system. An aluminum foil inside an evacuated aluminum can was used as thermal radiation shield. The cryostat temperature controller was calibrated prior to the experiment with the para/ferroelectric phase transition in KDP at 123 K. The temperature was stable within one degree during the experiment. No systematic variation in the intensities of three test reflections was found. All reflections were measured out to $\sin\theta/\lambda = 0{\cdot}69$ Å$^{-1}$ for one octant of the Ewald sphere. In addition, reflections were measured within the region $0{\cdot}69 < \sin\theta/\lambda < 1{\cdot}04$ Å$^{-1}$ for $|F_c|^2 \geq 2{\cdot}0$ (the structure factor calculation was based on the refined neutron-determined room-temperature structure with $\beta_{ij}$ values divided by 2·0), as well as some 550 symmetry-related reflections distributed over other octants. Several systematically extinct reflections were recorded in $\psi$ scans as a check on space-group assignment and multiple-scattering effects. No evidence of the latter was found. Second-order contamination was checked and found to be negligible. The background for each reflection was ascertained by the profile-analysis method (Lehmann & Larsen, 1974). Lorentz and absorption corrections (with a Gaussian grid of 10 × 6 × 14 points) were made. No averaging was made of symmetry-related reflections.

The experimental linear absorption coefficient was obtained by measuring the intensity attenuation of a strong reflection through a crystal positioned over a small hole in a Cd plate placed at the aperture to the detector. Repeated measurements were performed on several crystals. From the experimentally determined quantity, $\mu_{obs}$, a value of 37 (2) barn (1 barn $\equiv 10^2$ fm$^2$) was calculated for the incoherent (elastic + inelastic) scattering cross-section of H from the relation $\mu_{obs} = \sum N_i(\sigma_i^{\text{true abs}} + \sigma_i^{\text{incoh}})$, where $N_i$ is the number of atoms of element $i$ per cm$^3$ in the compound. The values of $\sigma_i^{\text{true abs}}$ (*International Tables for X-ray Crystallography*, 1968) used in the formula above were calculated at the experimental wavelength and $\sigma^{\text{incoh}}$ was taken to be 0·7 barn for Li, 0·3 barn for N and negligible for O (*International Tables for X-ray Crystallography*, 1974).

### *The* 295 K *data; data collection and reduction*

The room-temperature data were collected in two stages. All reflections *hkl* within one octant were measured out to $\sin\theta/\lambda = 0{\cdot}69$ Å$^{-1}$. The corre-

Table 2. *Neutron data collections*

| | 120 K | 295 K |
|---|---|---|
| Reactor | High-Flux Reactor at the Institut Laue–Langevin, Grenoble, France | R2 at AB Atomenergi, Studsvik, Sweden |
| Diffractometer | D9, four-circle diffractometer | Hilger & Watts PDP-8 controlled 4-circle diffractometer |
| Flux at sample | $3 \times 10^4$ n mm$^{-2}$ s$^{-1}$ | $9 \times 10^3$ n mm$^{-2}$ s$^{-1}$ |
| Monochromator | Cu(200), transmission | Cu(220), double monochromator system |
| $\lambda$ (Å) | 0·8317 (2) | 1·210 (4) |
| $\lambda/2$ contamination | 0·9% | <0·5% |
| Homogeneous beam area | 100 mm$^2$ | 100 mm$^2$ |
| Detector | $^3$He proportional counter | $^3$He proportional counter |
| Cooling device | Air Products and Chemicals Inc., one-stage closed-loop cryostat | |
| Temperature (K) | 120 (±1) | 295 (±1) |
| Scanning mode | $\omega$–$2\theta$ step scanning, 32 steps/reflection | $\omega$–$2\theta$ step scanning, 50 steps/reflection |
| Scan interval in $\theta$ | 2·0, 2·0, 2·4, 2·9, 3·6° for $\theta$ = 0, 15, 25, 40, 60° respectively | $\Delta\theta$ = 2·50° for all reflections |
| $(\sin\theta/\lambda)_{max}$ (Å$^{-1}$) | 1·04 | 0·69 |
| Number of test reflections | 3 | 3 |
| Number of reflections measured | 1468 | 821 |
| Number of reflections with $\lvert F_o\rvert^2 > 2\sigma_c(\lvert F_o\rvert^2)$ | 1328 | 670 |
| Number of unique reflections | 916 | 443 |
| Crystal volume (mm$^3$) | 7·4 | 25·6 |
| $\mu_{obs}$ (mm$^{-1}$) | 0·20 (1) | 0·22 (1) |
| $T$ range, absorption-weighted (mm) | 0·8–2·1 | 1·6–3·1 |
| Transmission range | 0·65–0·85 | 0·48–0·70 |
| Extinction level $(\lvert F_o\rvert^2_{uncorr} = y\lvert F_o\rvert^2_{corr})$ | 3% of reflections have $y < 0·85$ | 18% of reflections have $y < 0·85$ |

Table 3. *Agreement between symmetry-related reflections*

For the 120 K data set 551 symmetry-related pairs of reflections are compared, for the 295 K data 378 pairs.

| | | 120 K | 295 K |
|---|---|---|---|
| Before absorption correction: | $R$ | 2·5% | 7·2% |
| | $R_w$ | 2·9 | 8·3 |
| After absorption correction: | $R$ | 2·2 | 3·7 |
| | $R_w$ | 2·2 | 3·4 |
| After extinction correction: | $R$ | 2·1 | 2·5 |
| | $R_w$ | 2·9 | 3·5 |

sponding $\bar{h}kl$ reflections were measured at a later stage. The 66 $0kl$ reflections common to both sets of data had a discrepancy index (as defined in the next section) of <1%. A scale factor of 1·00 was thus assumed between the two data sets. The test reflections were stable. Profile analysis, Lorentz and absorption (10 × 8 × 8 grid) corrections were carried out as described earlier. Symmetry-related reflections were not averaged. The linear absorption coefficient was here measured directly with the primary beam emerging from the double-crystal monochromator. With the same procedure as above, the incoherent scattering cross-section for H was calculated to be 39 (2) barn. The quantities $\sigma_i^{incoh}$ in the expression above are sums of $\sigma_i^{incoh,\,elastic}$ and $\sigma_i^{incoh,\,inelastic}$. These quantities depend on the vibrational behavior of the element in question and on the wavelength used (see for example Marshall & Lovesey, 1971). Since the two experiments reported in this paper were carried out at different wavelengths and at different temperatures, it was not expected that the two values for $\sigma_H^{incoh}$ (and $\mu_{obs}$) would agree.

All calculations were carried out on IBM 370/155 and IBM 1800 computers with programs described by Lundgren (1979), except for the profile analysis of the 120 K data which was carried out on the PDP-10 computer at the Institut Laue–Langevin, Grenoble.

### Standard deviations and weights

For both data sets the weighting formula used in the least-squares minimization of $\sum w[\lvert F_o\rvert^2 - \lvert F_c\rvert^2]^2$ was $w^{-1} = \sigma^2(\lvert F_o\rvert^2) = \sigma_c^2(\lvert F_o\rvert^2) + k^2\lvert F_o\rvert^4$, where $\sigma_c^2$ was based on Poisson counting statistics and $k$ was empirically fixed to 0·010 and 0·015 for the low- and room-temperature refinements, respectively. For a successful refinement it is important that the weighting scheme used properly reflects the random errors (and also any remaining experimental systematic errors) in the observed structure factors. The variation of the test reflections and the agreement between symmetry-related reflections were analyzed in order to check the quality of the present two data sets and to obtain another estimate of $\sigma(\lvert F_o\rvert^2)$. This procedure is incap-

able of exposing *all* sources of systematic errors, however.

No systematic variations were found in the test reflections, and the random scatter was well described by $\sigma_c$. The agreement between symmetry-equivalent reflections may be expressed by $R = [\sum (|F_o|^2 - \langle|F_o|^2\rangle)^2/\sum |F_o|^4]^{1/2}$ or $R_w = [\sum w(|F_o|^2 - \langle|F_o|^2\rangle)^2/\sum w|F_o|^4]^{1/2}$, where $\langle|F_o|^2\rangle$ is the weighted average intensity of a symmetry-equivalent set of reflections. These indices are given in Table 3 for both data sets before absorption and extinction correction, after absorption correction only and after both absorption and extinction correction (*i.e.* after the least-squares refinements). The expression $w^{-1} = \sigma_c^2 + k^2|F_o|^4$ has been used in the latter case, but use of $w^{-1} = \sigma_c^2$ results in very similar values. It is seen that the discrepancy indices are already quite small for the 120 K data even before the absorption correction; this is a consequence of the similarity in the path lengths of the symmetry-related reflections.

An alternative check on data quality from symmetry-related reflections is to make a normal probability plot (Abrahams & Keve, 1971), in which all values of $\delta R = (|F_o|^2 - \langle|F_o|^2\rangle)/\sigma_c(|F_o|^2)$ for the data set are arranged in sequence and plotted against the expected normal distribution (Lundgren & Liminga, 1979). The result of such a plot was that the 120 K data (after absorption and extinction corrections) fell reliably on a straight line with slope 0·93 and intercept 0·01. The 295 K plot approximated almost as closely to a straight line with slope 0·90 and intercept 0·01. This suggests that Poisson counting statistics account satisfactorily for the scatter in the data set.

Table 4. *Refinements with different extinction models*

| Formalism* | Type | Distribution model† | $R_{w,F^2}$ (%) | Scale factor on $F_o$ |
|---|---|---|---|---|
| 120 K | | | | |
| No ext. corr. | – | – | 6·0 | 0·347 |
| B & C | I,iso. | Gaussian | 6·4 | 0·330 |
| B & C | I,iso. | Lorentzian | 4·8 | 0·330 |
| C & H | I,aniso. | Gaussian, C & H | 4·7 | 0·329 |
| B & C | I,aniso. | Gaussian, C & H | 4·7 | 0·330 |
| B & C | I,aniso. | Lorentzian, C & H | 4·7 | 0·329 |
| B & C | I,aniso. | Lorentzian, T & N | 4·7 | 0·329 |
| B & C | II,iso. | – | 4·9 | 0·334 |
| 295 K | | | | |
| C & H | iso. | – | 5·6 | 0·0254 |
| B & C | I,iso. | Gaussian | 8·4 | 0·0262 |
| B & C | I,iso. | Lorentzian | 6·2 | 0·0254 |
| C & H | I,aniso. | Gaussian, C & H | 4·7 | 0·0253 |
| B & C | I,aniso. | Gaussian, C & H | 4·3 | 0·0259 |
| B & C | I,aniso. | Gaussian, T & N | 4·5 | 0·0259 |
| B & C | I,aniso. | Lorentzian, C & H | 4·6 | 0·0252 |
| B & C | I,aniso. | Lorentzian, T & N | 4·5 | 0·0256 |
| B & C | II,iso. | – | 7·0 | 0·0269 |
| B & C | II,aniso. | – | 6·7 | 0·0272 |

* B & C refers to the Becker & Coppens (1974*a*,*b*, 1975) extinction formalism. C & H refers to the Coppens & Hamilton (1970) anisotropic modification of the Zachariasen (1967) extinction formalism.

† T & N refers to the angular mosaic distribution proposed by Thornley & Nelmes (1974).

## Extinction

Both data sets are affected quite seriously by extinction. With the definition $|F_o|^2_{\text{uncorr}} = y|F_o|^2_{\text{corr}}$, 3% of the 120 K data ($\lambda = 0{\cdot}8317$ Å) have $y$ values in the range $0{\cdot}67 < y < 0{\cdot}85$. For the 295 K data ($\lambda = 1{\cdot}210$ Å), 4·5% of the $y$ values lie in range $0{\cdot}34 < y < 0{\cdot}67$, and 13·4% in the range $0{\cdot}67 < y < 0{\cdot}85$. Several secondary-extinction models were tried for both data sets, and the results from these refinements are summarized in Table 4. The equivalent mosaic particle size as obtained from the isotropic type II refinements was $<10^{-3}$ mm for both data sets. The ratio $\bar{T}/\Lambda$, where $\Lambda$ is the extinction distance (see for example, Becker, 1977), was <0·005 for all reflections. This implies the validity of the kinematical theory for diffraction.

E.s.d.'s of refined parameters, $R$ values, conventional normal probability plots (for all reflections and for the most extinction-affected ones only) and agreement between symmetry-related reflections were used as criteria for the suitability of the extinction model in question.

Refinements with the low-temperature data appeared to be insensitive to the type of extinction model employed. Omission of an extinction correction, however, increased the scale factor on $|F_o|$ by 5%, and the normal probability plot acquired a more distinct curvature than with the isotropic models. As a check of the applicability of the extinction model to reflections in different $y$ ranges, the Becker & Coppens anisotropic Lorentzian type I formalism was applied to the data set for (*a*) all reflections, (*b*) the 31 reflections with $y < 0{\cdot}83$ removed, and (*c*) the 82 reflections with $y < 0{\cdot}91$ removed. One refinement was also made with only the 266 most extinction-affected reflections ($y < 0{\cdot}95$). In none of these cases was any significant change observed in the values of the refined positional and thermal parameters.

For the 295 K data set, it was found that: (*a*) the extinction was of type I, (*b*) the extinction was anisotropic and (*c*) all anisotropic type I models gave essentially equivalent results.

## Final refinements

In the final stages of refinement with the low-temperature data, all observed reflections were included except 17 reflections where $||F_o|^2 - |F_c|^2|/\sigma(F_o^2)$ was >6·0.

For these reflections, it was suspected that the vacuum lines to the cryostat could have interfered with the incident or reflected beam. In cases where symmetry-equivalent reflections had been measured, it could indeed be seen that the $|F_o|^2$ values agreed very poorly. The extinction model used was the Becker & Coppens type I formalism with Lorentzian anisotropic Coppens & Hamilton type mosaic-spread distribution.

In the final stages of refinement of the room-temperature data, all reflections with $y < 0.65$ (16 in total) were excluded. The same extinction model was chosen as for the 120 K data. Results from the refinements are presented in Tables 5, 6, 7 and 8.*

A scattering length of −1·94 fm is listed in *International Tables for X-ray Crystallography* (1974) for the natural isotope mixture of Li [7·42% of $^6$Li according to *Handbook of Chemistry and Physics*

* A list of structure factors has been deposited with the British Library Lending Division as Supplementary Publication No. SUP 35056 (17 pp.). Copies may be obtained through The Executive Secretary, International Union of Crystallography, 5 Abbey Square, Chester CH1 2HU, England.

Table 5. *Final refinement*

| | 120 K | 295 K |
|---|---|---|
| Total number of reflections in the refinement | 1436 | 775 |
| Number of reflections with $\|F_o\|^2 > 2\sigma(\|F_o\|^2)$ | 1267 | 645 |
| Number of parameters refined | 53 | 53 |
| Scale factor (on $F_o$)* | 0·326 (1) | 0·0252 (1) |
| $R_F$* | 4·2% | 4·1% |
| $R_{w,F^2}$ | 4·5% | 4·9% |
| $S$† | 1·59 | 1·54 |
| Extinction parameters ($\times 10^{-8}$) | | |
| $Z_{11}$ | 0·60 (6) | 1·49 (13) |
| $Z_{22}$ | 0·91 (11) | 0·59 (8) |
| $Z_{33}$ | 0·32 (2) | 0·51 (5) |
| $Z_{12}$ | 0·18 (7) | −0·15 (5) |
| $Z_{13}$ | −0·05 (3) | −0·26 (5) |
| $Z_{23}$ | 0·07 (3) | −0·10 (4) |
| Principal values and directions for the angular mosaic spread tensor | 3·3″ (0·41, 0·91, 0·06)<br>4·5″ (0·87, −0·37, −0·32)<br>6·1″ (0·27, −0·19, 0·95) | 2·6″ (0·97, −0·12, −0·23)<br>4·0″ (−0·02, 0·85, −0·54)<br>5·5″ (0·26, 0·52, 0·81) |

* Discrepancies between scale factors and $R$ values given here and in Table 4 follow from $|F_o|^2 < 2\sigma(|F_o|^2)$ reflections being omitted from the refinements in Table 4.

† $S = [\sum w(|F_o|^2 - |F_c|^2)^2/(m-n)]^{1/2}$, where $m$ is the total number of reflections and $n$ is the number of parameters refined.

Table 6. *Atomic coordinates* ($\times 10^5$)

The upper row refers to the 120 K data, the lower row to the 295 K data.

| | | $x$ | $y$ | $z$ |
|---|---|---|---|---|
| | Li | 0 | 0 | 0 |
| | N | 0 | 21656 (3) | 25000 |
| | | | 21763 (5) | |
| | O(1) | 0 | 16920 (4) | 6829 (9) |
| | | | 17030 (7) | 7014 (16) |
| | O(2) | 0 | 31603 (5) | 25000 |
| | | | 31610 (9) | |
| | O(3) | 28885 (7) | 47916 (4) | 25000 |
| | | 29027 (11) | 47835 (6) | |
| | O(4) | 0 | 64055 (6) | 25000 |
| | | | 63823 (11) | |
| $H_2O(3)$ | H(1) | 21347 (17) | 41467 (7) | 25000 |
| | | 21690 (27) | 41444 (12) | |
| | H(2) | 30804 (15) | 3582 (7) | 25000 |
| | | 30569 (22) | 3410 (12) | |
| $H_2O(4)$ | H(3) | 0 | 68587 (10) | 12146 (22) |
| | | | 68252 (17) | 12270 (36) |

Table 7. *Thermal parameters*

Mean-square amplitudes $U_{ij}$ are given in Å$^2$. The form of the anisotropic temperature factor is $\exp[-2\pi^2(U_{11}h^2a^{*2} + \ldots + 2U_{12}hka^*b^* + \ldots)]$. The r.m.s. components ($R_i$ in Å) along the principal axes of the thermal vibration ellipsoids are also listed. The upper row refers to the 120 K data. The lower row to the 295 K data.

| | $U_{11}$ | $U_{22}$ | $U_{33}$ | $U_{12}$ | $U_{13}$ | $U_{23}$ | $R_1$ | $R_2$ | $R_3$ |
|---|---|---|---|---|---|---|---|---|---|
| Li | 0·0157 (8) | 0·0175 (8) | 0·0139 (8) | 0 | 0 | 0·0000 (7) | 0·118 (4) | 0·125 (3) | 0·132 (3) |
| | 0·0359 (14) | 0·0397 (16) | 0·0242 (14) | | | 0·0016 (13) | 0·152 (5) | 0·187 (4) | 0·197 (4) |
| O(1) | 0·0273 (3) | 0·0138 (2) | 0·0128 (2) | 0 | 0 | 0·0005 (2) | 0·112 (1) | 0·118 (1) | 0·165 (1) |
| | 0·0685 (6) | 0·0311 (4) | 0·0303 (5) | | | 0·0000 (3) | 0·172 (1) | 0·175 (1) | 0·261 (1) |
| O(2) | 0·0171 (3) | 0·0075 (2) | 0·0376 (5) | 0 | 0 | 0 | 0·087 (1) | 0·131 (1) | 0·194 (1) |
| | 0·0435 (7) | 0·0195 (5) | 0·0754 (10) | 0 | 0 | 0 | 0·138 (2) | 0·207 (2) | 0·274 (2) |
| O(3) | 0·0125 (2) | 0·0118 (2) | 0·0116 (2) | −0·0016 (2) | 0 | 0 | 0·103 (1) | 0·108 (1) | 0·118 (1) |
| | 0·0305 (4) | 0·0286 (4) | 0·0269 (4) | −0·0037 (3) | 0 | 0 | 0·159 (1) | 0·163 (1) | 0·181 (1) |
| O(4) | 0·0182 (3) | 0·0165 (3) | 0·0157 (3) | 0 | 0 | 0 | 0·125 (1) | 0·129 (1) | 0·135 (1) |
| | 0·0455 (7) | 0·0383 (6) | 0·0372 (8) | | | | 0·191 (2) | 0·195 (2) | 0·213 (2) |
| N | 0·0127 (2) | 0·0077 (1) | 0·0165 (2) | 0 | 0 | 0 | 0·088 (1) | 0·113 (1) | 0·129 (1) |
| | 0·0327 (4) | 0·0189 (3) | 0·0360 (4) | | | | 0·139 (1) | 0·182 (1) | 0·191 (1) |
| H(1) | 0·0319 (5) | 0·0213 (4) | 0·0396 (6) | −0·0090 (4) | 0 | 0 | 0·127 (2) | 0·192 (1) | 0·199 (1) |
| | 0·0575 (9) | 0·0369 (8) | 0·0623 (10) | −0·0126 (7) | | | 0·174 (2) | 0·249 (2) | 0·251 (2) |
| H(2) | 0·0246 (4) | 0·0233 (4) | 0·0331 (5) | −0·0046 (3) | 0 | 0 | 0·139 (2) | 0·169 (1) | 0·182 (1) |
| | 0·0416 (7) | 0·0418 (7) | 0·0483 (7) | −0·0030 (6) | | | 0·195 (2) | 0·210 (2) | 0·219 (2) |
| H(3) | 0·0395 (6) | 0·0443 (6) | 0·0326 (6) | 0 | 0 | 0·0149 (5) | 0·150 (2) | 0·199 (1) | 0·234 (1) |
| | 0·0636 (10) | 0·0732 (12) | 0·0571 (12) | 0 | 0 | 0·0199 (11) | 0·206 (3) | 0·252 (2) | 0·295 (2) |

Table 8. *Interatomic distances* (Å) *and angles* (°) (*see Figs.* 1 *and* 2)

The upper row refers to the 120 K data, the lower row to the 295 K data. The e.s.d.'s include contributions from the e.s.d.'s in the cell parameters.

(*a*) $Li^+$ ion

| | | | |
|---|---|---|---|
| Li–O(3) | 2·075 (1) | O(3)–Li–O(3) | 93·82 (8) |
| | 2·088 (1) | | 93·82 (3) |
| Li–O(1) | 2·182 (1) | O(3)–Li–O(3) | 86·18 (8) |
| | 2·206 (1) | | 86·18 (3) |
| | | O(3)–Li–O(1) | 89·47 (2) |
| | | | 89·56 (3) |
| | | O(3)–Li–O(1) | 90·53 (2) |
| | | | 90·44 (3) |

(*b*) $NO_3^-$ ion

| | | | |
|---|---|---|---|
| N–O(1) | 1·239 (1) | O(1)–N–O(1) | 122·09 (7) |
| | 1·235 (1) | | 121·70 (9) |
| N–O(2) | 1·260 (1) | O(1)–N–O(2) | 118·95 (3) |
| | 1·252 (1) | | 119·15 (5) |

(*c*) $H_2O$ molecules: distances

| | O–H···O | O–H | O···O | H···O |
|---|---|---|---|---|
| $H_2O(3)$ | O(3)–H(1)···O(2) | 0·961 (1) | 2·834 (2) | 1·901 (2) |
| | | 0·953 (2) | 2·855 (1) | 1·933 (2) |
| | O(3)–H(2)···O(4) | 0·969 (1) | 2·818 (2) | 1·850 (1) |
| | | 0·964 (2) | 2·834 (1) | 1·871 (2) |
| $H_2O(4)$ | O(4)–H(3)···O(1) | | 3·069 (1) | 2·157 (1) |
| | | 0·958 (1) | 3·101 (1) | 2·200 (2) |
| | O(4)–H(3)···O(2) | 0·949 (2) | 3·034 (2) | 2·217 (2) |
| | | | 3·055 (1) | 2·236 (2) |

$H_2O$ molecules: angles

| | | |
|---|---|---|
| $H_2O(3)$ | H(1)–O(3)–H(2) | 106·0 (1) |
| | | 105·8 (2) |
| | O(3)–H(1)···O(2) | 162·9 (1) |
| | | 161·8 (2) |
| | O(3)–H(2)···O(4) | 178·0 (1) |
| | | 177·7 (1) |
| $H_2O(4)$ | H(3)–O(4)–H(3) | 106·4 (2) |
| | | 107·0 (3) |
| | O(4)–H(3)···O(1) | 158·5 (1) |
| | | 158·2 (2) |
| | O(4)–H(3)···O(2) | 142·6 (1) |
| | | 143·9 (2) |

(1971–1972)]. Bacon (1972) gives the value −2·14 fm. The isotope ratio $^6Li/^7Li$ in our bulk powder of $LiNO_3.3H_2O$ was measured on a mass spectrometer and found to correspond to a $^6Li$ content of 7·7 (±0·2)%. Refinement showed the mean scattering length for Li to be −1·95 (2) fm for the 120 K data and −1·96 (3) fm for the 295 K data. Refinement of the scattering length of N gave $b_N$ = 9·24 (3) fm for the 120 K data and 9·24 (5) fm for the 295 K data, in agreement with the mean experimental value of 9·17 (9) fm (Kvick, Koetzle, Thomas & Takusagawa, 1974), but slightly lower than the $b_N$ = 9·36 (2) fm quoted by Koester & Steyerl (1977). The scattering lengths used in the final least-squares refinements were $b_H$ = −3·72, $b_{Li}$ = −1·96, $b_N$ = 9·24 and $b_O$ = 5·75 fm. The following 53 parameters were refined: one scale factor, six anisotropic extinction parameters, positional and anisotropic thermal parameters for all atoms. The largest peaks in the $(F_o - F_c)$ residual maps calculated after the last cycles correspond to a scattering density of <2% of the maximum peak height for N in the $F_o$ synthesis maps.

The somewhat elongated shape of the thermal ellipsoid of O(2) of the nitrate group (see Table 7 and Fig. 2) (also observed in the X-ray studies) motivated trial refinements in the two other possible space groups, $C2cm$ and $Cmc2_1$, for the low-temperature data. Both refinements converged but the agreement factors were larger than for the centrosymmetric space group.

A higher-cumulant refinement (Johnson, 1969) for O(2) and for the H atoms was also attempted with the low-temperature data. The refined elements in the third-cumulant tensors were generally smaller than one e.s.d., however, and the agreement factors were not improved.

## The structure

The present neutron diffraction studies confirm the structure determined from the room-temperature X-ray experiment. The nitrate ion, $Li^+$ ion and one of the two independent water molecules lie in a mirror plane perpendicular to **a** (Fig. 1). Layers of this type are linked together by the second water molecule (Fig. 2). See Fig. 1 of Hermansson, Thomas & Olovsson (1977) for an illustration of the complete structure. Distances and angles at 120 and 295 K are presented in Table 8.

The Li–O and the O···O hydrogen-bond distances are seen to increase by 0·01–0·03 Å between 120 and 295 K. Since the layers in the structure are held together by such contacts, it is not surprising that the thermal expansion of the unit cell is largest along **a**, *i.e.* perpendicular to these layers. Both the N–O and O–H lengths become shorter as the temperature is raised. This is an artifact of an improper thermal model in

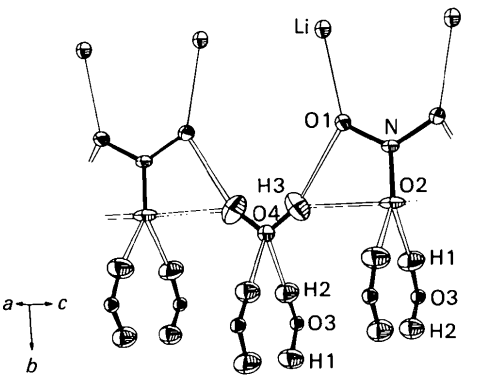


Fig. 1. The bonding around the $H_2O(4)$ water molecule at 120 K. O(4) occupies an *mm* symmetry site. Here and in Fig. 2 the thermal ellipsoids are drawn to include 50% probability.

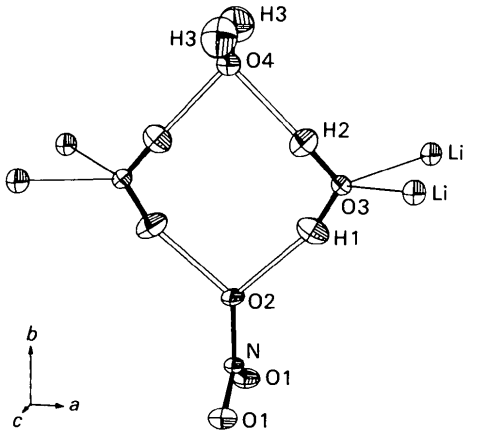


Fig. 2. The bonding around the $H_2O(3)$ molecule at 120 K. $H_2O(3)$ occupies an *m* symmetry site, the mirror plane lying roughly in the plane of the paper.

which particularly the librational motion is inadequately described. From IR data for $K_2C_2O_4.H_2O$ and $Ba(ClO_3)_2.H_2O$, Eriksson, Berglund, Tegenfeldt & Lindgren (1979) have calculated the corrections for systematic errors in the $H_2O$ geometry as obtained by neutron diffraction methods. They found the apparent rigid-body librational shortening of the O—H distance to be as large as 0·04 Å and the lengthening due to anharmonic stretching to be around 0·02 Å. The net effect of thermal motion is thus a shortening of the O—H length relative to the equilibrium value.

## Thermal motion

The thermal parameters are listed in Table 7.

The thermal ellipsoids of the nitrate atoms are markedly anisotropic. The elongated shape of the thermal ellipsoid of O(2) along **c** must largely be an effect of vibration rather than of disorder, since the value of $U_{33}$ for O(2) is twice as large at 295 as at 120 K. At 120 K, the thermal ellipsoids of both water O(3) and O(4) are fairly isotropic. The mean-square amplitudes out of the planes of the water molecules for the three H atoms are rather similar. Within the water-molecule planes, however, the mean-square amplitudes of the H atoms are much larger for $H_2O(4)$ than for $H_2O(3)$. The $Li^+$ ion motion is quite isotropic at 120 K, but distinctly anisotropic at room temperature.

From a comparison of the thermal parameters observed at the two different temperatures we found that:

(*a*) The mean-square amplitudes for the N and O atoms are, on the whole, proportional to temperature; with a few exceptions, the ratios $U_{ii}^{295}/U_{ii}^{120}$ for the N and O atoms lie in the range 2·25–2·60 (the temperature ratio is 2·46).

(*b*) For Li and, in particular, for the H atoms, the temperature dependence of the mean-square vibrational amplitudes is less; the $U_{ii}^{295}/U_{ii}^{120}$ ratios are 2·3 (1), 2·3 (1) and 1·7 (1) for Li, and lie in the range 1·46–1·80 for the H atoms.

It is of interest to consider the contribution of the various vibrational modes in the system to the observed temperature factors. In this way it may be possible to explain the temperature dependence of the thermal parameters.

The mean-square amplitudes of vibration $U_{ii}$ for a particular atom are obtained by summing over all normal vibrations. Within the harmonic approximation, the mass-weighted mean-square amplitude of a normal vibration with wavenumber $\bar{\nu}$ at temperature $T$ is given by [see for example Cyvin (1968)]

$$\langle Q^2 \rangle = \frac{h}{8\pi^2 c\bar{\nu}} \coth\left(\frac{hc\bar{\nu}}{2kT}\right) \qquad (1)$$

which becomes $(16{\cdot}8/\bar{\nu})\coth(0{\cdot}720\bar{\nu}/T)$ Å² a.m.u. when $\bar{\nu}$ is expressed in $cm^{-1}$ and $T$ in K. This function is plotted against $T$ for different wavenumbers in Fig. 3. It can be seen that only for very low wavenumbers is $\langle Q^2 \rangle$ closely proportional to $T$ (*i.e.* the dashed extrapolations of the curves in Fig. 3 approach zero) in the temperature range studied. According to (1), the theoretical upper limit for the atomic vibrational mean-square amplitude ratio $\langle u^2 \rangle^{295}/\langle u^2 \rangle^{120}$ is equal to the temperature ratio (2·46). For $\bar{\nu}$ equal to 50, 100,

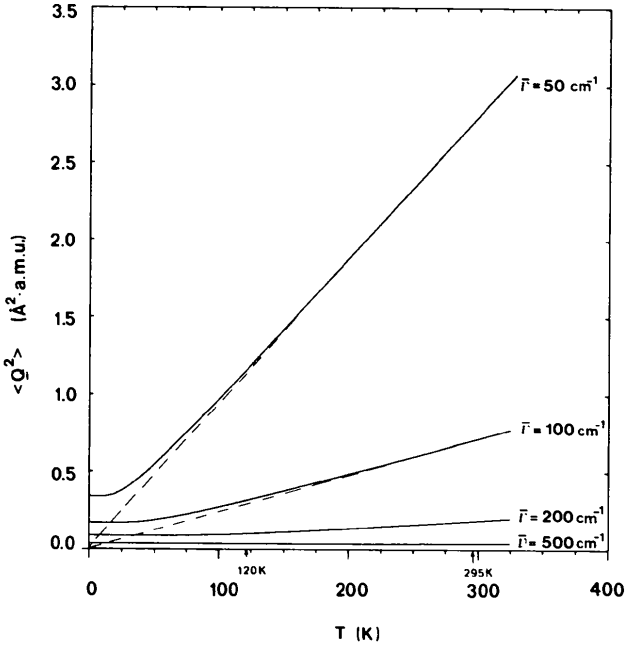


Fig. 3. The function $\langle Q^2 \rangle = (h/8\pi^2 c\bar{\nu})\coth(hc\bar{\nu}/2kT)$ plotted against temperature for various wavenumbers $\bar{\nu}$. Note: The masses of the vibrating species must be taken into account in transforming from $\langle Q^2 \rangle$ to $\langle u^2 \rangle$.

200, 300, 400, 500 and 700 $cm^{-1}$ this ratio is 2·40, 2·24, 1·84, 1·52, 1·31, 1·18 and 1·07, respectively.

IR spectroscopic data for $LiNO_3.3H_2O$ have been recorded at 100 K between 30 and 4000 $cm^{-1}$. From a comparison of the spectra for the normal and the deuterated compound, we found $H_2O$ librational vibrations at 510, 560, and 630 $cm^{-1}$. The low-frequency region for $LiNO_3.3H_2O$ was dominated by three broad absorption bands at 175, 230 and 330 $cm^{-1}$, and additional bands were found at 40, 105, 115 and 140 $cm^{-1}$. No normal coordinate analysis of these data has been attempted.

Instead, we shall, in the following, use information gathered from other normal coordinate analyses on compounds containing $H_2O$, $NO_3^-$ or $Li^+$, and consider, in turn, the vibrational behavior of these species.

IR spectroscopic data for water molecules in hydrates show absorption bands due to translational modes of vibration at 50–250 $cm^{-1}$, librations at 350–800 $cm^{-1}$, a bending mode around 1650 $cm^{-1}$ and stretching modes at 3200–3500 $cm^{-1}$.

Using a somewhat idealized model for the motion of a water molecule in a crystalline hydrate, we assumed that the six external rigid-body vibrations consist of three pure translational vibrations and three pure rock, wag and twist librations around the inertial axes. The contribution from these six modes to the experimentally observed $U_{ii}$ values for the atoms in the $H_2O(4)$ molecule in $LiNO_3.3H_2O$ at 120 K was calculated. The value 150 $cm^{-1}$ was taken as a typical wavenumber for translational motion; 600 $cm^{-1}$ was chosen for the rock, wag and twist librations. For the translations, (1) gives

$$\langle u^2 \rangle = \frac{16{\cdot}8}{m\tilde{\nu}} \coth\left(0{\cdot}720\,\frac{\tilde{\nu}}{T}\right) \qquad (2)$$

and for the librations

$$\langle \varphi^2 \rangle = \frac{16{\cdot}8}{I\tilde{\nu}} \coth\left(0{\cdot}720\,\frac{\tilde{\nu}}{T}\right) \qquad (3)$$

where $\langle u^2 \rangle$ is the mean-square amplitude in Å$^2$, $\langle \varphi^2 \rangle$ is the mean-square amplitude in rad$^2$, $m$ is the vibrating mass in a.m.u., and $I$ is the moment of inertia [1·775, 0·594 and 1·182 a.m.u. Å$^2$ for the rock, wag and twist librations of the $H_2O(4)$ molecule]. For O(4), the calculated values of $U_{ii}^{120}$ are 0·0087 Å$^2$ (translations only), and for H(3) $U_{11}^{120} = 0{\cdot}0350$, $U_{22}^{120} = 0{\cdot}0180$ and $U_{33}^{120} = 0{\cdot}0128$ Å$^2$ (translations and librations). Comparisons with Table 7 show that the translational and librational modes make a considerable contribution to the observed thermal ellipsoids of the water molecules. Differences between the observed and calculated mean-square amplitudes are to be expected because of the crudeness of the dynamic model employed.

It is not surprising that the observed temperature dependence is smaller for the H atoms in $LiNO_3.3H_2O$ than for the non-hydrogen atoms. For the H atoms, the librations (and to some extent the high-frequency internal modes) constitute a large part of the total mean-square amplitudes, and the temperature dependence for such modes is quite small.

The vibrational behavior of the nitrate ion in crystals is not as well studied as that of the water molecule. The internal modes for $NO_3^-$ lie above 700 $cm^{-1}$ (see for example Nakamoto, 1963). Concerning the librations and translations, Bon, Benoit & Bernard (1976) have measured IR and Raman spectra of $Sr(NO_3)_2$, $Ba(NO_3)_2$ and $Pb(NO_3)_2$ at different temperatures and assigned rotational vibrations of the $NO_3^-$ ions to bands found at 30 $cm^{-1}$ and 110–180 $cm^{-1}$. Translations of the $NO_3^-$ ions were found at 60, 130 and 210 $cm^{-1}$. An estimate of the mean-square vibration amplitudes of N, O(1) and O(2) in $LiNO_3.3H_2O$ from the above rotational and translational frequencies suggests that such highly temperature-dependent modes constitute a major contribution to the observed thermal ellipsoids.

Compounds containing the $Li^+$ ion show IR absorption bands at 350–500 $cm^{-1}$ due to translations of the $Li^+$ ion. From (2) with $\tilde{\nu} = 350$ $cm^{-1}$, the value 0·0071 Å$^2$ is obtained for the $U_{ii}^{120}$ values of Li. In $LiNO_3.3H_2O$ the experimentally observed $U_{ii}^{120}$ values (from Table 7) are 0·0157, 0·0175 and 0·0139 Å$^2$.

From the above discussion one would conclude that, at least as far as the nitrate ion and the water O atoms are concerned, low-frequency vibrational modes constitute a major part of the temperature factors. This results in a close proportionality between temperature and mean-square amplitude in the temperature range studied. For the water H atoms and the $Li^+$ ion, however, modes with a smaller temperature dependence also contribute significantly to the thermal ellipsoids.

We thank the staff of the ILL (Grenoble), in particular Dr M. S. Lehmann, for valuable help with the low-temperature experiment, and Dr R. Tellgren (Uppsala Univ.) for his help with the room-temperature data collection at Studsvik. We also thank Messrs John Allibon (ILL), H. Karlsson (Uppsala Univ.) and Sten Åhlin (Studsvik) for their expert technical assistance, Dr L. Nilsson for his help with the mass spectrometer measurements, Mr G. Olovsson for his assistance with the low-temperature data collection, and Drs A. Eriksson and J. Lindgren for valuable discussions concerning the interpretation of the thermal parameters. A. Eriksson also recorded the far-IR spectra of $LiNO_3.3H_2O$.

One of us (KH) thanks the Wallenberg Foundation for a travel grant.

This work has been supported by grants from the Swedish Natural Science Research Council.

### References

ABRAHAMS, S. C. & KEVE, E. T. (1971). *Acta Cryst.* A**27**, 157–165.

BACON, G. E. (1972). *Acta Cryst.* A**28**, 357–358.

BECKER, P. (1977). *Acta Cryst.* A**33**, 243–249.

BECKER, P. & COPPENS, P. (1974*a*). *Acta Cryst.* A**30**, 129–147.

BECKER, P. & COPPENS, P. (1974*b*). *Acta Cryst.* A**30**, 148–153.

BECKER, P. & COPPENS, P. (1975). *Acta Cryst.* A**31**, 417–425.

BON, A. M., BENOIT, C. & BERNARD, O. (1976). *Phys. Status Solidi B*, **78**, 67–78.

COPPENS, P. & HAMILTON, W. C. (1970). *Acta Cryst.* A**26**, 71–83.

CYVIN, S. J. (1968). *Molecular Vibrations and Mean Square Amplitudes*, p. 78. Trondheim: Universitetsforlaget.

ERIKSSON, A., BERGLUND, B., TEGENFELDT, J. & LINDGREN, J. (1979). *J. Mol. Struct.* **52**, 107–112.

*Handbook of Chemistry and Physics* (1971–1972). Cleveland: Chemical Rubber Publishing Company.

HERMANSSON, K., THOMAS, J. O. & OLOVSSON, I. (1977). *Acta Cryst.* B**33**, 2857–2861.

HERMANSSON, K., THOMAS, J. O. & OLOVSSON, I. (1980). To be published.

*International Tables for X-ray Crystallography* (1968). Vol. III, 2nd ed., p. 197. Birmingham: Kynoch Press.

*International Tables for X-ray Crystallography* (1974). Vol. IV, p. 270. Birmingham: Kynoch Press.

JOHNSON, C. K. (1969). *Acta Cryst.* A**25**, 187–194.

KOESTER, L. & STEYERL, A. (1977). *Neutron Physics*, p. 36. Berlin, Heidelberg, New York: Springer.

KVICK, Å., KOETZLE, T. F., THOMAS, R. & TAKUSAGAWA, F. (1974). *J. Chem. Phys.* **60**, 3866–3874.

LEHMANN, M. S. & LARSEN, F. K. (1974). *Acta Cryst.* A**30**, 580–584.

LUNDGREN, J.-O. (1979). *Crystallographic Computer Programs*. Report UUIC-B13-04-04, Institute of Chemistry, Univ. of Uppsala.

LUNDGREN, J.-O. & LIMINGA, R. (1979). *Acta Cryst.* B**35**, 1023–1027.

LUNDGREN, J.-O. & TAESLER, I. (1979). *Acta Cryst.* B**35**, 2384–2386.

MARSHALL, W. & LOVESEY, S. W. (1971). *Theory of Thermal Neutron Scattering*. Oxford Univ. Press.

NAKAMOTO, K. (1963). *Infrared Spectra of Inorganic and Coordination Compounds*. New York, London: John Wiley.

THORNLEY, F. R. & NELMES, R. J. (1974). *Acta Cryst.* A**30**, 748–757.

ZACHARIASEN, W. H. (1967). *Acta Cryst.* **23**, 558–564.


*Acta Cryst.* (1980). B**36**, 1040–1044

# Structure de l'Oxyde de Plomb et de Rhodium $Pb_3Rh_7O_{15}$


PAR JEAN OMALY ET ROBERT KOHLMULLER

*Laboratoire de Chimie Minérale, Université de Clermont* II, *BP* 45, *F* 63170 *Aubière, France*

PATRICK BATAIL

*Laboratoire de Cristallochimie, UER Sciences, F* 35031 *Rennes CEDEX, France*

ET RAYMOND CHEVALIER

*Laboratoire de Cristallographie et Physico-Chimie des Matériaux Université de Clermont* II, *BP* 45, *F* 63170 *Aubière, France*


(*Reçu le* 17 *juin* 1979, *accepté le* 1 *janvier* 1980)


### Abstract

The synthesis of $Pb_3Rh_7O_{15}$ and its structure determined by X-ray diffraction methods are described. The material crystallizes in the hexagonal space group $P6_3/mcm$ with $a = 10{\cdot}342\ (2)$, $c = 13{\cdot}270\ (6)$ Å, $Z = 4$ and $d_c = 8{\cdot}64$ Mg m$^{-3}$. The final $R$ value is 0·044 for 591 independent reflexions. $Rh^{4+}$ ions are in 6($f$) sites and statistically distributed with $Rh^{3+}$ in 12($i$) sites.


0567-7408/80/051040-05$01.00

### Introduction

Le système PbO–$Rh_2O_3$ en présence d'air a fait l'objet de peu d'études. Cependant Sleight (1971) signale l'existence d'une phase $Pb_2^{4+}Rh_2^{3+}O_7$ obtenue sous pression. Gravier (1974) étudiant le système à 1173 K en vue d'employer PbO comme fondant pour l'élaboration de rhodite indique à cette température la présence d'une phase hexagonale de groupe Laue